Acta Crystallographica Section C
Crystal Structure Communications
ISSN 0108-2701

Nimustine hydrochloride: the first crystal structure determination of a 2-chloroethyl-*N*-nitrosourea hydrochloride derivative by X-ray powder diffraction and solid-state NMR

Sándor L. Bekö,[a] David Urmann,[a] Andrea Lakatos,[b] Clemens Glaubitz[b] and Martin U. Schmidt[a]*

[a]Institute of Inorganic and Analytical Chemistry, Goethe University, Max-von-Laue Strasse 7, D-60438 Frankfurt am Main, Germany, and [b]Institute of Biophysical Chemistry, Goethe University, Max-von-Laue Strasse 9, D-60438 Frankfurt am Main, Germany
Correspondence e-mail: m.schmidt@chemie.uni-frankfurt.de

Received 14 September 2011
Accepted 6 February 2012
Online 24 February 2012

Nimustine hydrochloride [systematic name: 4-amino-5-({[*N*-(2-chloroethyl)-*N*-nitrosocarbamoyl]amino}methyl)-2-methylpyrimidin-1-ium chloride], $C_9H_{14}ClN_6O_2^+\cdot Cl^-$, is a prodrug of CENU (chloroethylnitrosourea) and is used as a cytostatic agent in cancer therapy. Its crystal structure was determined from laboratory X-ray powder diffraction data. The protonation at an N atom of the pyrimidine ring was established by solid-state NMR spectroscopy.

Comment

The human brain has a special membrane, known as the blood–brain barrier (BBB), that protects it very efficiently from foreign substances. These include the vast majority of drugs used in cancer therapy. Drug therapy of brain tumours is therefore difficult to carry out and the range of suitable cytostatic agents (those which inhibit or suppress cellular growth and multiplication) is severely restricted. Every year, most disconcertingly, more than 800 000 new cases in which the central nervous system is afflicted with cancer are registered worldwide. The majority of these cases involve brain tumours, as shown by the latest study by the Robert Koch Institute (Husmann *et al.*, 2010).

A study carried out by Skipper *et al.* (1961) drew attention to research on nitrosoureas. Of all tested cytostatics, measurable efficiency against brain tumours could only be observed for 1-methyl-1-nitrosourea (the only representative of the nitrosoureas in the aforementioned study). Since then, a range of nitrosourea derivatives has been synthesized and extensively examined (Johnston *et al.*, 1966). Some of them, for example carmustine (or BiCNU or BCNU, from bis-chloroethylnitrosourea) and lomustine (or CeeNU or CCNU, from chloroethylcyclonitrosourea), showed very high efficacy against tumours and were able to cross the BBB. However, their low solubility in water limited their application (Kanamaru *et al.*, 1980). In 1972, the Central Research Laboratory, Sankyo Co. Ltd, Tokyo, synthesized further nitrosourea derivatives, including the title nimustine hydrochloride [systematic name: 4-amino-5-({[*N*-(2-chloroethyl)-*N*-nitrosocarbamoyl]-amino}methyl)-2-methylpyrimidin-1-ium chloride], (I), which is not only soluble in water but can also pass through the BBB (Nakao *et al.*, 1972). Nimustine hydrochloride is currently marketed under the trade name Nidran (or ACNU, from aminopyrimidinechloroethylnitrosourea). Currently, (I) belongs to the group of standard drugs in the fight against brain tumours, where contemporary therapeutic schemes also include radiation and surgical removal of the tumour (Kamiryo *et al.*, 2004).

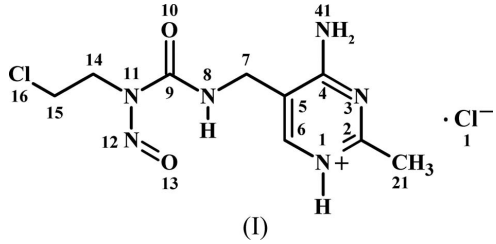

(I)

The exact mechanism of action is currently still under investigation. However, preliminary findings indicate that DNA is directly attacked by alkylation of the guanine blocks at the O^6 position to yield O^6-(2-chloroethyl)guanine. This alkylation massively affects the function of DNA because, in contrast with guanine, O^6-(2-chloroethyl)guanine prefers to build up base pairs with thymine instead of cytosine. The information stored in the DNA is altered and thereby successful replication and transcription are prevented. However, the possibility of repairing the alkylated guanine blocks using the body's own enzyme O^6-alkylguanine DNA alkyltransferase still exists. If this process does not happen, or occurs too slowly, the affected DNA strands may be damaged almost irreversibly. The O^6-(2-chloroethyl)guanine formed is unstable and can react *via* the intramolecularly formed intermediate N^1,O^6-ethanoguanine with the complementary DNA strand to form 1-(3-cytosinyl)-2-(1-guanosinyl)ethane. As a consequence, both DNA strands are covalently crosslinked. The resulting double-strand breaks are considerably more difficult to repair, thus usually leading to cell death. However, the body is known to possess its own mechanisms able to repair even these double-strand breaks. These mechanisms are currently under investigation in the hope that, with the knowledge thus accumulated, the efficacy of agents such as nimustine hydrochloride can be increased (Kobayashi *et al.*, 1994; Margison & Santibáñez-Koref, 2002; Batista *et al.*, 2007; Kondo *et al.*, 2010). The expectation is that the elucidation of the exact crystal structure of nimustine hydrochloride, determined from X-ray powder diffraction and solid-state NMR spectroscopy and reported here, will provide additional momentum to the investigation of the mode of action of nitrosourea derivatives as cytostatics and the body's response

  doi:10.1107/S0108270112005252

to them, as well as to the development of new prodrug candidates.

Preliminary thermogravimetric analysis (TGA) showed no mass loss or gain up to 426 K, indicating that the lattice of (I) contains no solvent or water molecules. The onset of weight loss occurred at 428 K, and differential scanning calorimetry (DSC) showed a sharp exothermic signal at 428 K attributed to decomposition.

Protonation can occur at any of four possible positions (N1, N3, N8 and N41) in (I). H-atom positions are generally difficult to determine by X-ray powder diffraction, although there have been cases when they have been determined successfully (Schmidt *et al.*, 2011), even from laboratory powder data (Bekö *et al.*, 2010). In this instance, the position of the protonation could be determined by solid-state NMR spectroscopy using cross-polarization magic-angle spinning (CPMAS). In the ^{15}N CP MAS spectrum, only the hydrogen-carrying N atoms could be detected. Three ^{15}N peaks were observed, which, on the basis of their chemical shifts (referenced against liquid ammonia), were assigned to the $-NH_2$ (N41, 91.55 p.p.m.), –NH (N8, 102.98 p.p.m.) and aromatic NH^+ (N1 or N3, 172.79 p.p.m.) moieties. By comparing the ^{15}N chemical-shift values with those obtained by Städeli & von Philipsborn (1980) for aminopyrimidines in different protonation states in solution, it can be unambiguously concluded that the chemical shift value of 172.79 p.p.m. [which corresponds to −207.44 p.p.m. when spectra are referenced against nitromethane, as in the paper of Stadeli & von Philipsborn (1980)] for the aromatic N atom certainly indicates a protonated positively charged state. However, this measurement did not allow a decision to be reached on whether the protonation had occurred at N1 or N3.

Solution NMR studies on pyridine and pyrimidine derivatives show that protonation of the ring N atom strongly affects the ^{13}C chemical shifts of the adjacent C atoms (Riand *et al.*, 1977; Liu *et al.*, 1991). Thus, it seemed reasonable to use ^{13}C NMR for the determination of the protonation site on the pyrimidine ring. Due to the low natural abundance of ^{13}C isotopes, no correlation experiments could be performed in the solid state. Therefore, resonance assignments were made based on the ^{13}C solution NMR spectrum recorded in d_6-DMSO (perdeuterated dimethyl sulfoxide), since the signals in the two spectra (solid state and solution) have similar chemical shifts (see Table 2). The ^{13}C signals in d_6-DMSO were assigned using heteronuclear single-quantum correlation (HSQC) and heteronuclear multiple-bond correlation (HMBC) experiments.

Through a comparison of the ^{13}C chemical shifts of neutral (in d_6-DMSO) and monoprotonated (in trifluoroacetic acid, TFA) pyrimidine derivatives, Riand *et al.* (1974) were able to show that the C atoms adjacent to protonated N atoms become more shielded and thus their signals undergo upfield shifts compared with the neutral molecule. These upfield shifts are larger for a C atom attached to an H atom than for one attached to a methyl group. Riand *et al.* (1974) also determined that, in the case of 4-aminopyrimidines, monoprotonation occurs almost completely on atom N1 *para* to the amino group. Protonation of N1 in the case of 4-amino-2-methylpyrimidine has the strongest effect on C6, for which the chemical shift changes from 154.75 to 144.8 p.p.m. The signal of the methyl group at position 2 also undergoes an upfield shift from 25.57 to 21.4 p.p.m. A similar ∼10 p.p.m. upfield shift of the C6 resonance was observed for 4-amino-5-methylpyrimidine (from 153.5 to 142.2 p.p.m.) due to protonation at N1. Consequently, the chemical shift of C6 could also be an indicator for the protonation state of N1 in the case of nimustine hydrochloride, and its value at 141.8 p.p.m. strongly suggests that N1 is protonated. A prediction of the ^{13}C chemical shifts of the neutral and differently protonated nimustine molecules using the program *CHEMDRAW Ultra 12.0* from CambridgeSoft Corporation (Cousins, 2011) provided further substantiation for this finding. Since the software was not able to perform calculations with protonated N atoms, we used the *N*-methylated form to create the positive charge. The effect of an *N*-methyl substituent on the ^{15}N, ^{13}C and ^{1}H chemical shifts is very similar to that of an H atom (Liu *et al.*, 1991). The results are summarized in Table 2. The chemical shifts obtained for the N1-methylated derivative show the best agreement with the solid-state NMR data, which again indicates that (I) is protonated at N1.

For the crystal structure determination of nimustine hydrochloride from laboratory X-ray powder diffraction data, the diffractogram was recorded in transmission mode on a Stoe STADI-P diffractometer with a Ge(111) monochromator and a linear position-sensitive detector using Cu $K\alpha_1$ radiation. The sample was measured for 52 h in a 0.7 mm capillary in a 2:1 ratio with amorphous SiO_2 to minimize preferred orientation, since (I) crystallizes in small tablet-like crystals, as shown in Fig. 1. The software *WinXPOW* (Stoe & Cie, 2004) was used for data acquisition.

For indexing and structure solution, the powder pattern was truncated to a real-space resolution of approximately 3.4 Å, which for Cu $K\alpha_1$ radiation corresponds to the range 3.0–26.5° in 2θ. The background was subtracted with a Bayesian high-

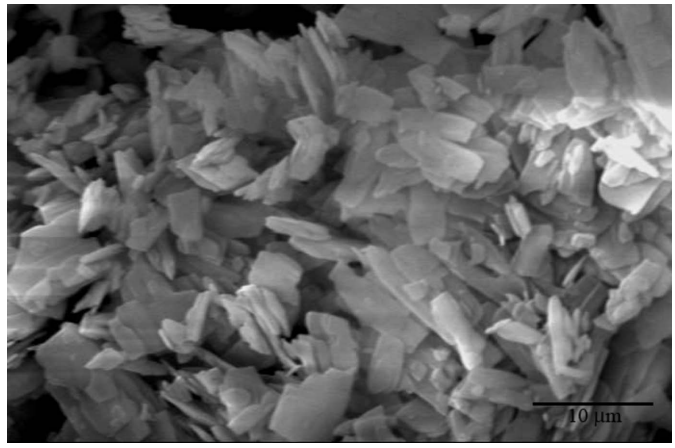

Figure 1
A scanning electron microscopy image of nimustine hydrochloride, (I), showing the tabular habit of the crystals.

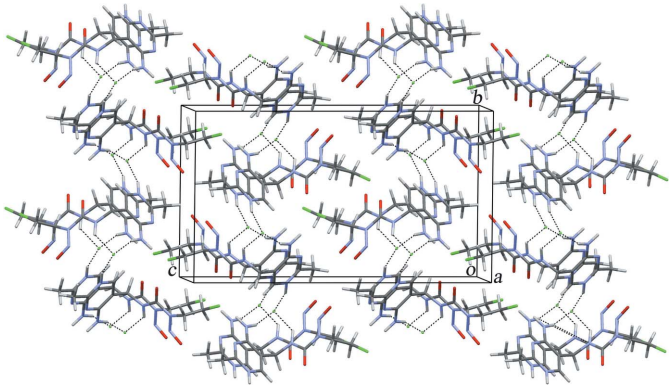

Figure 2
A packing diagram for (I), showing the zigzag arrangement and double-layer packing motif along the crystallographic *c* axis. Hydrogen bonds running parallel to the *b* axis are represented with dashed lines.

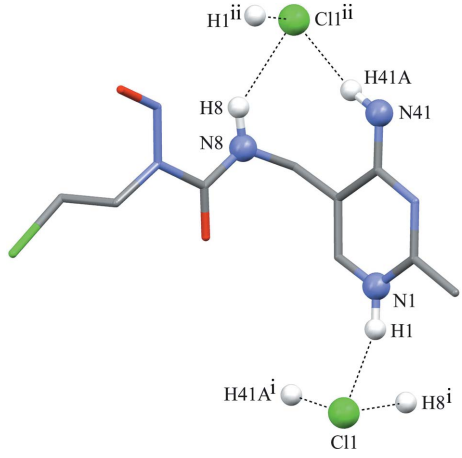

Figure 3
A view of the hydrogen bonds (dashed lines) to the neighbouring molecules of (I). All H atoms not taking part in hydrogen bonds have been omitted for clarity. [Symmetry codes: (i) $-x, y+\frac{1}{2}, -z+\frac{1}{2}$; (ii) $-x, y-\frac{1}{2}, -z+\frac{1}{2}$.]

pass filter (David & Sivia, 2001). The powder pattern could be indexed without ambiguity with the program *DICVOL91* (Boultif & Louër, 1991), resulting in a monoclinic unit cell with $V = 1370$ Å^3. A comparison of the unit-cell volume with Hofmann's volume increments (Hofmann, 2002) led to the estimation that $Z = 4$. Subsequently, a Pawley (1981) refinement was carried out to extract the integrated intensities and their correlations, converging with a Pawley χ^2 value of 2.29. From the refinement, the space group was determined to be $P2_1/c$ using Bayesian statistical analysis (Markvardsen *et al.*, 2001). The crystal structure was solved from the powder pattern in direct space with simulated annealing using the program *DASH 3.1* (David *et al.*, 2006). The H atoms were included (see *Experimental*). The starting molecular geometry was taken from the single-crystal structure of 1-(2-chloroethyl)-3-(*trans*-4-methylcyclohexyl)-1-nitrosourea, known as semustine (or MeCCNU, from methylchloroethylcyclonitrosourea) [Cambridge Structural Database (CSD; Version 5.32, updated November 2011; Allen, 2002) refcode CEMCNU10; Smith & Camerman, 1978], replacing the 4-methylcyclohexyl group with a 4-amino-2-methylpyrimidin-1-ium-5-yl group, which was constructed with bond lengths C—H = 1.089 Å, C—C alkyl = 1.530 Å, C—C aromatic = 1.384 Å, C—N aromatic = 1.338 Å, C—N amine = 1.468 Å and N—H amine = 1.015 Å, using the program *Mercury* (Macrae *et al.*, 2008). Two models were constructed, one with the protonation at N1 and one with it at the N3 position.

The nimustine molecule has seven flexible torsion angles, which were left free during the simulated annealing (rotations around single bonds, except for C—NH_2 and C—CH_3). In 50 simulated annealing runs, the crystal structure was found approximately ten times for both models. Both models resulted in the same chloride anion position, close to the N1 position, with N1···Cl distances typical for an N—H···Cl hydrogen bond (Allen, 2002). This confirmed atom N1 to be protonated, as shown by the NMR experiments, and gave the final indication for further development of this model.

The nimustine molecules in (I) show a zigzag arrangement along the crystallographic *c* axis. They are bridged by chloride anions *via* hydrogen bonds formed with the primary amine substituent of the pyrimidine, the secondary amine group of the urea and the protonated N atom of the pyrimidine fragment, leading to a chain-like motif along the crystallographic *b* axis. The three NH groups form a channel around the chloride anions which runs parallel to the *a* axis (Fig. 2). Each nimustine molecule is connected to two different chloride anions (Table 1 and Fig. 3).

Experimental

Nimustine hydrochloride, (I), was purchased from Sigma–Aldrich (>98% purity) and used as received. The TGA measurement was performed on a SETARAM TGA 92 device. About 10–15 mg of the sample was filled into corundum crucibles and measured from room temperature to 473 K at a rate of 3 K min^{-1} under a nitrogen atmosphere. The DSC measurement was performed on a SETARAM DSC 131 device in a similar fashion as for the TGA measurement. For the solid-state NMR measurements, 80 mg of crystalline (I) with a natural ^{15}N and ^{13}C isotope abundance was used. The compound was packed in a 4 mm zirconia rotor. The measurements were performed on a Bruker 850 MHz instrument at 10 kHz spinning speed at 290 K and referenced against liquid ammonia. The ^{13}C NMR spectrum was measured on a Bruker Avance 400 device in tubes filled with d_6-DMSO (reference) and 15–20 mg of (I). The scanning electron microscopy image in Fig. 1 was recorded using an Amray 1919 ECO scanning electron microscope at 20 kV and a low vacuum of 7 Pa. The elemental analysis (CHNS) was carried out on an Elementar (Vario MICRO cube) elemental analyser. About 1–4 mg of the sample was placed in a tin vessel and measured at 1423 K under a helium atmosphere with addition of oxygen during the measurement. Elemental analysis calculated for $C_9H_{14}Cl_2N_6O_2$ (%): C 34.97, H 4.56, N 27.18; found: C 34.98, H 4.54, N 27.17.

Crystal data

$C_9H_{14}ClN_6O_2^+\cdot Cl^-$
$M_r = 309.16$
Monoclinic, $P2_1/c$
$a = 5.25191$ (12) Å
$b = 12.2401$ (3) Å
$c = 21.4088$ (5) Å
$\beta = 93.2353$ (7)°
$V = 1374.05$ (6) Å^3
$Z = 4$
Cu $K\alpha_1$ radiation
$\lambda = 1.54056$ Å
$\mu = 4.35$ mm^{-1}
$T = 293$ K
Cylinder, 10 × 0.7 mm

Table 1
Hydrogen-bond geometry (Å, °).

D—H···A	D—H	H···A	D···A	D—H···A
N1—H1···Cl1	0.90	2.19	3.058 (3)	161.5
N8—H8···Cl1^{ii}	0.90	2.48	3.22 (3)	139.4
N41—H41A···Cl1^{ii}	0.87	2.29	3.22 (3)	160.8

Table 2
Comparison of the ^{13}C solid-state and ^{13}C liquid NMR measurements of (I) and the predicted values.

	Experimental values		Predicted values		
Atom	Solid state	In d_6-DMSO	Neutral	N1—CH$_3$†	N3—CH$_3$†
C21	21.7	21.3	24.5	19.9	23.2
C7	39.0	37.9	41.2	40.2	35.3
C14	40.1	39.9	40.3	40.3	40.3
C15	42.0	40.3	38.9	38.9	38.9
C5	110.9	112.1	112.7	108.0	136.0
C6	148.4	141.8	158.9	145.6	121.2
C9	153.56	153.9	153.0	153.0	153.0
C2	161.1	160.9	163.9	169.6	164.0
C4	164.7	163.5	161.4	164.0	164.5

† See *Comment*.

Data collection

Stoe STADI-P diffractometer with a linear position-sensitive detector
Specimen mounting: 0.7 mm glass capillary
Data collection mode: transmission
Scan method: step
$2\theta_{min}$ = 2.0°, $2\theta_{max}$ = 79.99°, $2\theta_{step}$ = 0.01°

Refinement

R_p = 0.087
R_{wp} = 0.084
R_{exp} = 0.061
R_{Bragg} = 0.012
χ^2 = 1.388
7600 data points
86 parameters
42 restraints
H-atom parameters not refined

The whole powder pattern out to 1.20 Å resolution was used for the Rietveld refinement. A total of 86 parameters were refined, namely the background (fitted using Chebyshev polynomials with 20 refinable coefficients), zero-point error, scale parameter, atomic coordinates (refined with restraints), anisotropic peak broadening, lattice parameters, a scale factor and a common isotropic displacement parameter for the C, N and O atoms. The isotropic displacement parameter of the H atoms was constrained at 1.2 times the global isotropic displacement parameter. For the two Cl atoms, individual isotropic displacement parameters were assigned. 42 suitable chemical restraints from *Mogul* (Bruno *et al.*, 2004) were added (see Table 3), 18 for bond lengths, 23 for bond angles and one for the planarity of the 4-amino-2-methylpyrimidin-1-ium-5-yl group, including the aromatic C and N, the amino N and the methyl and alkyl C atoms. Finally, the H-atom positions were adjusted using the *DREIDING*/*X6* force field (Mayo *et al.*, 1990) within the program package *Cerius*^{2} (Accelrys, 2003). During the optimization, the coordinates of all other atoms and the lattice parameters were fixed, as was the orientation of the H atoms of the methyl group attached to C2 on the pyrimidine ring. In the case of the methyl group attached to C2 of the pyrimidine ring, the H atoms had to be moved to a more suitable orientation with respect to the amine N1—H1 group. Bond lengths were fixed according to mean values from the CSD (aromatic C—H = 0.950 Å, methyl C—H = 0.969 Å, alkyl C—H = 0.985 Å,

Table 3
Restraints for bond lengths (Å) and angles (°), and flatten (°) and refined values from the refinement of (I).

Bond	Restraint value	Refined value	Angle	Restraint value	Refined value
N1—C2	1.343	1.351 (3)	C2—N1—C6	118.4	120.7 (2)
N1—C6	1.338	1.355 (2)	N1—C2—N3	121.6	121.4 (2)
C2—N3	1.313	1.336 (2)	N1—C2—C21	119.2	118.8 (2)
C2—C21	1.486	1.486 (3)	N3—C2—C21	119.2	119.8 (2)
N3—C4	1.338	1.358 (2)	C2—N3—C4	120.0	120.1 (2)
C4—C5	1.384	1.414 (2)	N3—C4—C5	120.0	119.3 (1)
C4—N41	1.335	1.330 (3)	N3—C4—N41	120.0	119.4 (2)
C5—C6	1.384	1.367 (3)	C5—C4—N41	120.0	121.3 (2)
C5—C7	1.530	1.527 (3)	C4—C5—C6	120.0	118.9 (1)
C7—N8	1.462	1.449 (4)	C4—C5—C7	120.0	122.8 (1)
N8—C9	1.324	1.322 (4)	C6—C5—C7	120.0	118.3 (2)
C9—O10	1.213	1.216 (4)	N1—C6—C5	120.0	119.6 (2)
C9—N11	1.381	1.407 (3)	C5—C7—N8	112.8	115.4 (2)
N11—N12	1.333	1.350 (4)	C7—N8—C9	120.6	119.5 (2)
N11—C14	1.481	1.487 (4)	N8—C9—O10	126.6	124.9 (3)
N12—O13	1.217	1.231 (5)	N8—C9—N11	114.5	114.3 (2)
C14—C15	1.446	1.461 (4)	O10—C9—N11	118.9	120.8 (3)
C15—Cl16	1.831	1.839 (4)	C9—N11—N12	118.3	118.4 (2)
			C9—N11—C14	119.9	119.7 (2)
			N12—N11—C14	121.8	121.3 (2)
			N11—N12—O13	114.7	116.7 (3)
			N11—C14—C15	108.8	107.8 (3)
			C14—C15—Cl16	106.5	108.0 (2)
Planar restraint†					
N1, C2, C21, N3, C4, C41, C5, C7, C6	0.0	4.6 (2)			

† See *TOPAS* manual (Coelho, 2007) for formulae.

primary amine N—H = 0.865 Å and secondary amine N—H = 0.898 Å). The difference electron density was calculated using *SHELXTL* (Sheldrick, 2008). The highest residual electron density (0.41 e Å^{-3}) is located close to the position of the chloride anion. However, a refinement of split-atom positions for Cl1 did not improve the fit. The final Rietveld plot for (I) is shown in Fig. 4.

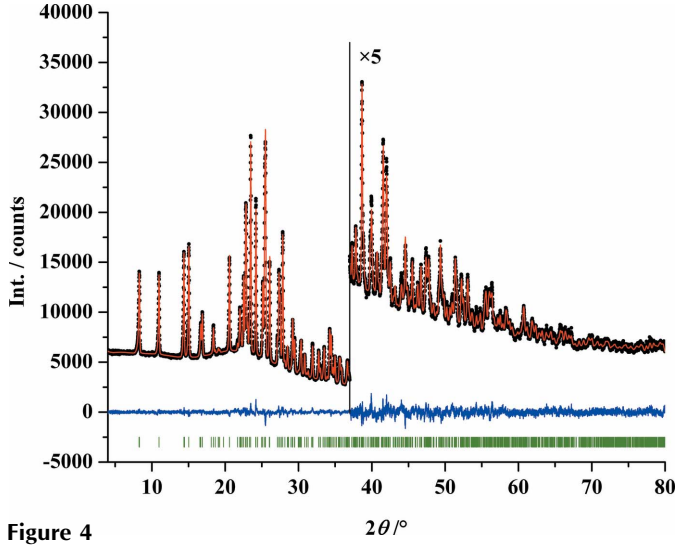

Figure 4
The final Rietveld plot, showing the observed (black points), calculated (upper solid line) and difference (lower solid line) profiles, and tick marks (vertical lines) indicating the calculated peak positions for (I). The change of scale at 37° in 2θ is a factor of five.

Data collection: *WinXPOW* (Stoe & Cie, 2004); cell refinement: *TOPAS Academic* (Coelho, 2007); data reduction: *DASH* (David *et al.*, 2006); program(s) used to solve structure: *DASH*; program(s) used to refine structure: *TOPAS Academic*; molecular graphics: *Mercury* (Macrae *et al.*, 2008); software used to prepare material for publication: *publCIF* (Westrip, 2010).

Supplementary data for this paper are available from the IUCr electronic archives (Reference: LG3071). Services for accessing these data are described at the back of the journal.

References

Accelrys (2003). *Cerius*^{2}. Accelrys Ltd, Cambridge, England.
Allen, F. H. (2002). *Acta Cryst.* B**58**, 380–388.
Batista, L. F. Z., Roos, W. P., Christmann, M., Menck, C. F. M. & Kaina, B. (2007). *Cancer Res.* **67**, 11886–11895.
Bekö, S. L., Thoms, S. D., Brüning, J., Alig, E., van de Streek, J., Lakatos, A., Glaubitz, C. & Schmidt, M. U. (2010). *Z. Kristallogr.* **225**, 382–387.
Boultif, A. & Louër, D. (1991). *J. Appl. Cryst.* **24**, 987–993.
Bruno, I. J., Cole, J. C., Kessler, M., Luo, J., Motherwell, W. D. S., Purkis, L. H., Smith, B. R., Taylor, R., Cooper, R. I., Harris, S. E. & Orpen, A. G. (2004). *J. Chem. Inf. Comput. Sci.* **44**, 2133–2144.
Coelho, A. A. (2007). *TOPAS Academic User Manual*. Coelho Software, Brisbane, Australia.
Cousins, K. R. (2011). *J. Am. Chem. Soc.* **133**, 8388.
David, W. I. F., Shankland, K., van de Streek, J., Pidcock, E., Motherwell, W. D. S. & Cole, J. C. (2006). *J. Appl. Cryst.* **39**, 910–915.
David, W. I. F. & Sivia, D. S. (2001). *J. Appl. Cryst.* **34**, 318–324.
Hofmann, D. W. M. (2002). *Acta Cryst.* B**58**, 489–493.
Husmann, G., Kaatsch, P., Katalinic, A., Bertz, J., Haberland, J., Kraywinkel, K. & Wolf, U. (2010). *Krebs in Deutschland 2005/2006 – Häufigkeiten und Trends*, 7. Ed. Berlin: Robert Koch Institut und die Gesellschaft der epidemiologischen Krebsregister in Deutschland.
Johnston, T. P., McCaleb, G. S., Opliger, P. S. & Montgomery, J. A. (1966). *J. Med. Chem.* **9**, 892–911.
Kamiryo, T., Tada, K., Shiraishi, S., Shinojima, N., Kochi, M. & Ushio, Y. (2004). *Neurosurgery*, **54**, 349–357.
Kanamaru, R., Asamura, M., Sato, H., Saito, S., Wakui, A. & Saito, T. (1980). *Tohoku J. Exp. Med.* **132**, 431–441.
Kobayashi, T., Tominaga, T. & Yoshimoto, T. (1994). *J. Neurooncol.* **22**, 23–31.
Kondo, N., Takahashi, A., Mori, E., Noda, T., Su, X., Ohnishi, K., McKinnon, P. J., Sakaki, T., Nakase, H., Ono, K. & Ohnishi, T. (2010). *Cancer Sci.* **101**, 1881–1885.
Liu, M., Farrant, R. D., Lindon, J. C. & Barraclough, P. (1991). *Spectrosc. Lett.* **24**, 1115–1121.
Macrae, C. F., Bruno, I. J., Chisholm, J. A., Edgington, P. R., McCabe, P., Pidcock, E., Rodriguez-Monge, L., Taylor, R., van de Streek, J. & Wood, P. A. (2008). *J. Appl. Cryst.* **41**, 466–470.
Margison, G. P. & Santibáñez-Koref, M. F. (2002). *Bioessays*, **3**, 255–266.
Markvardsen, A. J., David, W. I. F., Johnson, J. C. & Shankland, K. (2001). *Acta Cryst.* A**57**, 47–54.
Mayo, S. L., Olafson, B. D. & Goddard, W. A. III (1990). *J. Phys. Chem.* **94**, 8897–8909.
Nakao, H., Arakawa, M. & Fukushima, M. (1972). US Patent No. 4003901.
Pawley, G. S. (1981). *J. Appl. Cryst.* **14**, 357–361.
Riand, J., Chenon, M. T. & Lumbroso-Bader, N. (1974). *Tetrahedron Lett.* **36**, 3123–3126.
Riand, J., Chenon, M. T. & Lumbroso-Bader, N. (1977). *J. Am. Chem. Soc.* **99**, 6838–6845.
Schmidt, M. U., Brüning, J., Hützler, W. M., Mörschel, P., Ivashevskaya, S. N., van de Streek, J., Braga, D., Maini, L., Chierotti, M. R. & Gobetto, R. (2011). *Angew. Chem. Int. Ed.* **50**, 7924–7926.
Sheldrick, G. M. (2008). *Acta Cryst.* A**64**, 112–122.
Skipper, H. E., Schabel, F. M., Trader, M. W. & Thomson, J. R. (1961). *Cancer Res.* **21**, 1154–1164.
Smith, H. W. & Camerman, A. (1978). *J. Med. Chem.* **21**, 468–471.
Städeli, W. & von Philipsborn, W. (1980). *Helv. Chim. Acta*, **63**, 504–522.
Stoe & Cie (2004). *WinXPOW*. Stoe & Cie GmbH, Darmstadt, Germany.
Westrip, S. P. (2010). *J. Appl. Cryst.* **43**, 920–925.